NUCLEAR THEORY, Vol. 38 (2019)
eds. M. Gaidarov, N. Minkov, Heron Press, Sofia

Spin Dependent *Ab Initio* Nonlocal No-Core Shell-Model One-Body Densities

G. Popa[1], **M. Burrows**[2], **Ch. Elster**[2], **K.D. Launey**[3], **P. Maris**[4], **S.P. Weppner**[5]

[1]Ohio University, Zanesville OH 43701, USA
[2]Ohio University, Athens, OH 45701, USA
[3]Louisiana State University, Baton Rouge, LA 70803, USA
[4]Iowa State University, Ames, Iowa 50011, USA
[5]Eckerd College, St. Petersburg, Florida 33711, USA

Abstract. Constructing microscopic effective interactions ('optical potentials') for nucleon-nucleus (NA) elastic scattering requires in first order off-shell nucleon-nucleon (NN) scattering amplitudes between the projectile and the struck target nucleon and nonlocal one-body density matrices. While the NN amplitudes and the *ab intio* no-core shell-model (NCSM) calculations always contain the full spin structure of the NN problem, one-body density matrices used in traditional microscopic folding potential neglect spin contributions inherent in the one-body density matrix. Here we derive and show the expectation values of the spin-orbit contribution of the struck nucleon with respect to the rest of the nucleus for ^{4}He, ^{6}He, ^{12}C, and ^{16}O and compare them with the scalar one-body density matrix.

1 Introduction

The *ab-initio* NCSM has considerably advanced our understanding and capability of achieving first-principles descriptions of low-lying states in light nuclear systems [1–5], and has over the last decade taken center stage in the development of microscopic tools for studying the structure of atomic nuclei. Applying this approach to nuclear reactions requires isolating important degrees of freedom, thus reducing the many-body to a few-body problem and solving the latter exactly. Isolating important degrees of freedom means projecting onto a reduced Hilbert space and thus creating effective interactions between the degrees of freedom that are treated exactly. Since the 1960's (or earlier), such effective interactions have been constructed by fitting relevant experimental data with usually complex functions, leading to the well known phenomenological optical potentials (see e.g. [6–8]), which are local and energy-dependent. While the large body of phenomenological work may keep some place in practical applications, an overarching goal is to construct such effective interactions (optical potentials) from the same first principles that govern advances in many-body approaches to nuclear structure.

Starting from a multiple scattering expansion for NA scattering, the first order term requires a folding integral over a nonlocal one-body density and off-shell NN scattering amplitudes, where the Wolfenstein amplitude A determines the central part of the folding potential and C the spin-orbit part (see e.g. [9–12]). Calculations in [13,14] are carried out in this spirit. Here the non-local one-body density matrix (OBDM) and the NN scattering amplitudes are based on the same NN interaction, leading to a consistent *ab initio* first order folding effective potential.

However, 'traditional' first order folding potentials developed in the 1990s and used in [13,14] assume spin-saturation in nuclei and thus are most applicable to closed shell nuclei. Starting from a NCSM, even a closed shell nucleus is not spin-saturated; e.g. a fully converged calculation for ^{4}He requires $\mathrm{N}_{\max} \geq 12$, where $N_{\max}$ is defined as the maximum number of oscillator quanta above the valence shell for that nucleus. Though it is expected that closed shell nuclei are almost spin-saturated, this will certainly not be the case for nuclei with partially filled shells. In order to take into account the spin of the struck nucleon a formulation to extract one-body scalar and spin-densities from *ab initio* OBDMs needs to be developed. The scalar density is the one used in the 'traditional' folding interactions. From the spin-dependent densities, expectation values of the scalar product of spin $\boldsymbol{\sigma}_i$ of the struck target nucleon with the momenta inherent in the nonlocal one-body density must be evaluated consistently with the operator structure of the NN Wolfenstein amplitudes. A first step in this direction was made in [15] using a simple model density. Here we present scalar and spin-dependent OBDMs extracted from NCSM calculations.

2 Theoretical Framework

The NN scattering amplitude $\overline{M}$ can be parameterized according to Wolfenstein [16] in terms of six linearly independent spin-momentum operators multiplied by scalar functions of three linearly independent momentum vectors. The three vectors are the momentum transfer $\mathbf{q}$, the total momentum of the system $\boldsymbol{\mathcal{K}}_{NN}$, and the normal to the scattering plane $\mathbf{n}_{NN}$,

$$\begin{aligned}
\overline{M}(\boldsymbol{q},\boldsymbol{\mathcal{K}}_{NN},\epsilon) &= \\
&= A(\boldsymbol{q},\boldsymbol{\mathcal{K}}_{NN},\epsilon)\mathbf{1}\otimes\mathbf{1} + iC(\boldsymbol{q},\boldsymbol{\mathcal{K}}_{NN},\epsilon)(\boldsymbol{\sigma}^{(0)}\otimes\mathbf{1}+\mathbf{1}\otimes\boldsymbol{\sigma}^{(i)})\cdot\hat{n} \\
&+ M(\boldsymbol{q},\boldsymbol{\mathcal{K}}_{NN},\epsilon)(\boldsymbol{\sigma}^{(0)}\cdot\hat{n})\otimes(\boldsymbol{\sigma}^{(i)}\cdot\hat{n}) \\
&+ (G(\boldsymbol{q},\boldsymbol{\mathcal{K}}_{NN},\epsilon) - H(\boldsymbol{q},\boldsymbol{\mathcal{K}}_{NN},\epsilon))(\boldsymbol{\sigma}^{(0)}\cdot\hat{q})\otimes(\boldsymbol{\sigma}^{(i)}\cdot\hat{q}) \\
&+ (G(\boldsymbol{q},\boldsymbol{\mathcal{K}}_{NN},\epsilon) + H(\boldsymbol{q},\boldsymbol{\mathcal{K}}_{NN},\epsilon))(\boldsymbol{\sigma}^{(0)}\cdot\hat{\mathcal{K}})\otimes(\boldsymbol{\sigma}^{(i)}\cdot\hat{\mathcal{K}}) \\
&+ D(\boldsymbol{q},\boldsymbol{\mathcal{K}}_{NN},\epsilon)\left[(\boldsymbol{\sigma}^{(0)}\cdot\hat{q})\otimes(\boldsymbol{\sigma}^{(i)}\cdot\hat{\mathcal{K}}) + (\boldsymbol{\sigma}^{(0)}\cdot\hat{\mathcal{K}})\otimes(\boldsymbol{\sigma}^{(i)}\cdot\hat{q})\right], \quad (1)
\end{aligned}$$

where the scalar functions (A, C, M, G, H, and D) are the Wolfenstein amplitudes. The amplitude D is zero on-shell due to parity conservation. The mo-

menta are given as

$$\begin{aligned}\hat{q} &= \frac{(\boldsymbol{k}' - \boldsymbol{k})}{|\boldsymbol{k}' - \boldsymbol{k}|} \\ \widehat{\mathcal{K}} &= \frac{(\boldsymbol{k}' + \boldsymbol{k})}{|\boldsymbol{k}' + \boldsymbol{k}|} \\ \hat{n} &= \frac{\boldsymbol{\mathcal{K}} \times \boldsymbol{q}}{|\boldsymbol{\mathcal{K}} \times \boldsymbol{q}|} \,,\end{aligned} \tag{2}$$

with $\boldsymbol{k}$ and $\boldsymbol{k}'$, the initial and final momentum of the projectile nucleon. A spin-dependent space-fixed (sf) nonlocal one-body density between an initial A-body wave function $|\Psi\rangle$ and a final A-body wave function $|\Psi'\rangle$, is written as:

$$(\rho_{sf})^{K_s}_{q_s}(\boldsymbol{r}, \boldsymbol{r'}) = \left\langle \Psi' \left| \sum_{i=1}^{A} \delta^3(\boldsymbol{r_i} - \boldsymbol{r}) \delta^3(\boldsymbol{r'_i} - \boldsymbol{r'}) \left(\hat{\boldsymbol{\tau}}_{(i)}\right)^{K_s}_{q_s} \right| \Psi \right\rangle \,, \tag{3}$$

where $\boldsymbol{r_i}$ and $\boldsymbol{r'_i}$ are the initial and final space coordinate of the particle i, and $\boldsymbol{r}, \boldsymbol{r}'$ are parameters. Here $\hat{\boldsymbol{\tau}}_{(\boldsymbol{i})}$ is the one body spin operator acting on particle i, a spherical tensor of rank $K_s = 0, 1$. When $K_s = 0$, the spin operator becomes the identity operator.

$$\begin{aligned} K_s = 0 \quad &: \quad \left(\hat{\boldsymbol{\tau}}_{(\boldsymbol{i})}\right)^0_0 = \quad 1 \\ K_s = 1 \quad &: \quad \left(\hat{\boldsymbol{\tau}}_{(\boldsymbol{i})}\right)^1_0 = \quad \boldsymbol{\sigma}_z \\ &: \quad \left(\hat{\boldsymbol{\tau}}_{(\boldsymbol{i})}\right)^1_{-1} = \quad \frac{1}{\sqrt{2}} (\boldsymbol{\sigma}_x - i\boldsymbol{\sigma}_y) \\ &: \quad \left(\hat{\boldsymbol{\tau}}_{(\boldsymbol{i})}\right)^1_1 = \quad -\frac{1}{\sqrt{2}} (\boldsymbol{\sigma}_x + i\boldsymbol{\sigma}_y) \,. \end{aligned} \tag{4}$$

In order to remove the center-of-mass (c.m.) contribution, the non-local one-body density matrix is evaluated in momentum space, where we can employ the scheme given in detail in Ref. [17]. As function of the momentum variables $\boldsymbol{p}$ and $\boldsymbol{p}'$ the one-body density matrix $(\rho_{sf})^{K_s}_{q_s}(\boldsymbol{p}, \boldsymbol{p'})$ reads

$$\begin{aligned}(\rho_{sf})^{K_s}_{q_s}(\boldsymbol{p}, \boldsymbol{p'}) = &\sum_{nljn'l'j'} \sum_{K_l=|l-l'|}^{l+l'} \sum_{k_l=-K_l}^{K_l} \sum_{Kk} \langle K_l k_l K_s q_s | K k \rangle \\ &\times (-1)^{J'-M'} \begin{pmatrix} J' & K & J \\ -M' & k & M \end{pmatrix} \mathcal{Y}^{*ll'}_{Kk}(\hat{p}, \hat{p}') \\ &\times (-1)^{-l} \hat{j}\hat{j}'(K_s+1)\hat{s}\hat{K}_s\hat{K}_l \begin{Bmatrix} l' & l & K_l \\ s & s & K_s \\ j' & j & K \end{Bmatrix} R_{n'l'}(p') R_{nl}(p) \\ &\times (-i)^{l+l'} \left\langle A\lambda' J' || (a^\dagger_{n'l'j'} \tilde{a}_{nlj})^{(K)} || A\lambda J \right\rangle \,. \end{aligned} \tag{5}$$

The term $(a^\dagger_{n'l'j'}\tilde{a}_{nlj})^{(K)}$ represents the single particle transition operator of rank K, with $\hat{K} = \sqrt{2K+1}$, and the corresponding reduced matrix elements are characterized by the initial and final total angular momenta, J and J', while the remaining quantum numbers are summarized by λ, and λ'. These reduced matrix elements are provided by NCSM calculations.

To obtain translationally invariant densities we introduce as variables the momentum transfer $\boldsymbol{q}$ and the total momentum $\boldsymbol{\mathcal{K}}$,

$$\begin{aligned} \boldsymbol{q} &= \boldsymbol{p}' - \boldsymbol{p} \\ \boldsymbol{\mathcal{K}} &= \frac{1}{2}(\boldsymbol{p}' + \boldsymbol{p}) \,. \end{aligned} \tag{6}$$

The spin-dependent one-body density (SOBD) is then derived in the same fashion as outlined in [17], and we arrive at

$$\begin{aligned} (\rho_{sf})^{K_s}_{q_s}(\boldsymbol{q},\boldsymbol{\mathcal{K}}) = &\sum_{nljn'l'j'} \sum_{K_l=|l-l'|}^{l+l'} \sum_{k_l=-K_l}^{K_l} \sum_{Kk} \langle K_l k_l K_s q_s | K k\rangle \\ &\times (-1)^{J'-M'} \begin{pmatrix} J' & K & J \\ -M' & k & M \end{pmatrix} (-1)^{-l}\hat{j}\hat{j}'(K_s+1)\hat{s}\hat{K}_s\hat{K}_l \\ &\times \begin{Bmatrix} l' & l & K_l \\ s & s & K_s \\ j' & j & K \end{Bmatrix} (-i)^{l+l'} \\ &\times \sum_{n_q,n_\mathcal{K},l_q,l_\mathcal{K}} \langle n_\mathcal{K} l_\mathcal{K}, n_q l_q : K_l | n'l', nl : K_l\rangle_{d=1} R_{n_\mathcal{K} l_\mathcal{K}}(\mathcal{K}) R_{n_q l_q}(q) \\ &\times \mathcal{Y}^{*l_\mathcal{K} l_q}_{K_l k_l}(\hat{q},\hat{\mathcal{K}}) \left\langle A\lambda' J' \middle|\middle| (a^\dagger_{n'l'j'}\tilde{a}_{nlj})^{(K)} \middle|\middle| A\lambda J \right\rangle \,. \end{aligned} \tag{7}$$

In order to determine the center of mass (c.m.) contribution, we follow the same procedure as in [17]. The center of mass wavefunction is assumed to be entirely in the 0s ground state of the nucleus. This results in the term $\zeta_{c.m.}$ being 0 for the c.m. contribution. Thus, using the relative coordinates from Eq. (6) and c.m. decomposition given by $|\Psi\rangle = |\Psi_{int}\rangle \times |\Psi_{c.m.}0s\rangle$ we can separate the c.m. contribution and obtain the translational invariant part of the density. We obtained the center of mass contribution to be the same as in the scalar density.

3 Expectation Values of Spin Dependent One-Body Density

In order to evaluate the scattering amplitude of Eq. (1), expectation values of operators involving the struck target nucleon, represented by the scalar product of $\boldsymbol{\sigma}^{(i)}$ with one of the momentum vectors, must be calculated. If this operator is the unit operator, the result is a nonlocal scalar density, as e.g. used to calculate the effective NA interaction in Ref. [13]. The term proportional to the Wolfenstein amplitude A leads to the central part of the effective potential and the one proportional to C to its spin-orbit part when scattering from a spin-zero nucleus is considered. In general, the terms containing the scalar product of $\boldsymbol{\sigma}^{(i)}$

with the momentum vectors of Eq. (2) need to be evaluated in the c.m. frame of the nucleus. In the following, we will show explicit expressions for the expectation value of $\boldsymbol{\sigma}^{(i)} \cdot \hat{n}_{t.i}$, which is the momentum space representation of the spin-operator. The subscript $t.i.$ indicates that we use target c.m. momenta. We define

$$\begin{aligned}\mathcal{S}_n(\mathbf{r},\mathbf{r}') &= \left\langle \Phi' \left| \sum_{i=1}^{A} \delta^3(\mathbf{r_i}-\mathbf{r})\delta^{\mathbf{3}}(\mathbf{r'_i}-\mathbf{r}) \left[\boldsymbol{\sigma}^{(\mathbf{i})}\cdot\hat{\mathbf{n}}\right]_{\mathbf{0}}^{\mathbf{0}} \right| \Phi \right\rangle \\ &= \left\langle \Phi' \left| \sum_{i=1}^{A} \delta^3(\mathbf{r_i}-\mathbf{r})\delta^3(\mathbf{r'_i}-\mathbf{r}) \left[{\boldsymbol{\tau}_{(\boldsymbol{i})}}^{K_s=1}\cdot\hat{\boldsymbol{n}}^{1}_{\boldsymbol{t.i.}}\right]_0^0 \right| \Phi \right\rangle . \end{aligned} \quad (8)$$

Here spherical components of the spin tensor $\tau_{(\mathbf{i})}$ are used and coupled with components of $\hat{\mathbf{n}}_{\mathbf{t.i.}}$ to a tensor of rank 0. We rewrite $\mathcal{S}_n(\mathbf{r},\mathbf{r}')$ in terms of variables $\mathbf{q}$ and $\mathcal{K}$ following the same procedure as in Eq. (7). The final expression, after expanding the projection, becomes

$$\begin{aligned}&\mathcal{S}_n(\boldsymbol{q},\boldsymbol{\mathcal{K}}) = \\ &\sum_{q_s}(-1)^{-q_s}\langle 1q_s1-q_s|00\rangle \frac{4\pi}{3} \sum_{nljn'l'j'} \sum_{K_l=|l-l'|}^{l+l'} \sum_{k_l=-K_l}^{K_l} \sum_{Kk} \langle K_l k_l 1 q_s | K k\rangle \\ &(-1)^{J'-M'} \begin{pmatrix} J' & K & J \\ -M' & k & M \end{pmatrix} (-1)^{-l}\hat{j}\hat{j}'(2)\hat{s}\hat{1}\hat{K}_l \begin{Bmatrix} l' & l & K_l \\ s & s & 1 \\ j' & j & K \end{Bmatrix} \\ &(-i)^{l+l'} \sum_{n_q,n_{\mathcal{K}},l_q,l_{\mathcal{K}}} \langle n_{\mathcal{K}} l_{\mathcal{K}}, n_q l_q : K_l | n'l', nl : K_l\rangle_{d=1} R_{n_{\mathcal{K}}l_{\mathcal{K}}}(\mathcal{K}) R_{n_q l_q}(q) \\ &\sum_{LN}\langle K_l k_l 1 q_s | LN\rangle \sum_{ww'} \frac{1}{(4\pi)^2} \hat{l_q}\hat{l_{\mathcal{K}}}\hat{1}\hat{1}\hat{K}_l\hat{1} \langle l_q 010|w'0\rangle \langle l_{\mathcal{K}}010|w0\rangle \\ &\begin{Bmatrix} l_q & 1 & w' \\ l_{\mathcal{K}} & 1 & w \\ K_l & 1 & L \end{Bmatrix} \mathcal{Y}^{w'w}_{LN}(\hat{q},\hat{\mathcal{K}}) \left\langle A\lambda' J' \left|\left| (a^\dagger_{n'l'j'}\tilde{a}_{nlj})^{(K)} \right|\right| A\lambda J \right\rangle . \end{aligned} \quad (9)$$

While we concentrated in Eq. (8) on the expectation value of $\boldsymbol{\sigma}^{(i)} \cdot \hat{n}$, expressions for the expectation values of the other scalar products of $\boldsymbol{\sigma}^{(i)}$ with the unit vectors $\hat{q}$ and $\hat{\mathcal{K}}$ can be derived in a similar fashion. However, we notice that those expressions are scalar products between a pseudo-vector and a vector, which are not invariant under parity transformations. Thus, their expectation values between the ground states vanish, a fact we numerically verified.

For numerical studies, we only need to concentrate on the expectation values represented by Eq. (9), which we want to call spin-orbit density. We contrast the scalar nonlocal one-body density (K_s=0) with the density function given by the expectation value of the spin-orbit operator (K_s=1) in the ground state of the nucleus, which we call spin-orbit density.

The first example given in Figure 1 shows the two cases for the closed-shell nucleus ^{4}He and the open-shell nucleus ^{6}He. The expectation values of the

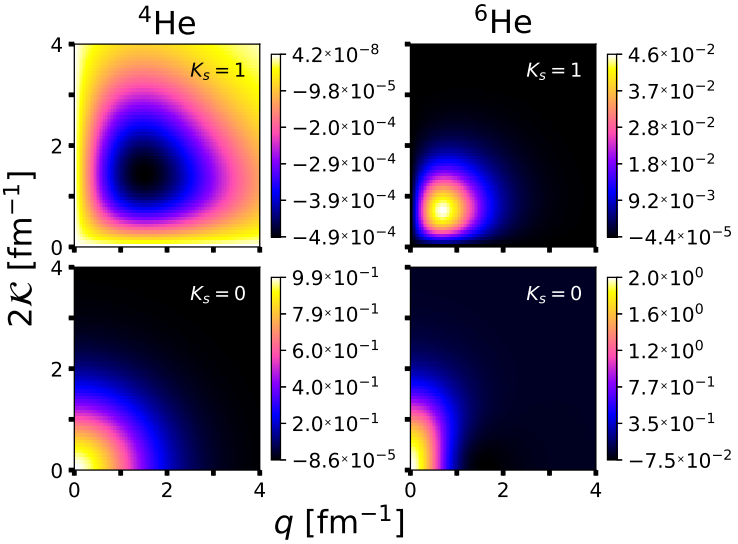

Figure 1. The expectation value of the scalar translationally invariant nonlocal one-body density ($K_s = 0$) and the spin-orbit operator ($K_s = 1$) as function of q and $\mathcal{K}$, with the angle between them fixed at 90^o, and evaluated in the ground state. All four graphs use one body reduced matrix elements from NCSM calculations with $N_{\max}$=18 and $\hbar\omega$=20 MeV based on the NNLO$_{\rm opt}$ interaction [18] for the neutron distribution of ^{4}He (left panels) and ^{6}He (right panels).

scalar translationally invariant nonlocal one-body density ($K_s = 0$) and the spin-orbit density ($K_s = 1$) as function of $\mathbf{q}$ and $\boldsymbol{\mathcal{K}}$, with the angle between them fixed at 90^o, are evaluated in the ground state of the corresponding nuclei. All four graphs use as input one body reduced matrix elements from NCSM calculations with $N_{\max} = 18$ and $\hbar\omega = 20$ MeV based on the NNLO$_{\rm opt}$ interaction [18] for the neutron distribution of ^{4}He (left panels) and ^{6}He (right panels). For ^{4}He, the spin-orbit contribution to the density is at least three orders of magnitude smaller than the scalar part. It is still interesting to notice that its maximum strength is at about $q = 1.5$ fm^{-1}, and $2\mathcal{K} = 1.5$ fm^{-1}, away from the maximum value of the scalar part that is at $q = 0$ and $\mathcal{K} = 0$. For ^{6}He, the maximum value of the spin-orbit contribution is only two order of magnitude smaller than the contribution from the scalar one. In this case, its maximum strength is at about $q = 0.7$ fm^{-1}, and $2\mathcal{K} = 0.7$ fm^{-1} away from $q = 0$ and $\mathcal{K} = 0$ where the maximum of the scalar density is located. This does show the importance of the spin-orbit contribution to the density in an open-shell nucleus like ^{6}He.

To further investigate the effect of the spin-orbit contribution to the density, we present the expectation value of the scalar translationally invariant nonlocal one-body density ($K_s = 0$) and the spin-orbit operator ($K_s = 1$) as function of

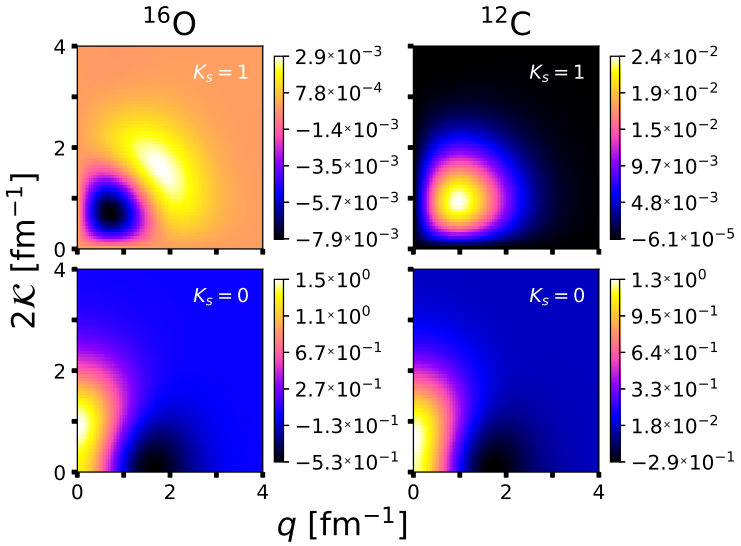

Figure 2. Same as Figure 1 but comparing the neutron distribution of ^{16}O (left panels) and ^{12}C (right panels). The NCSM calculations were performed at $N_{\max}$=10 and $\hbar\omega$=20 MeV using the NNLO$_{\rm opt}$ interaction [18].

$\mathbf{q}$ and $\mathcal{K}$, with the angle between them fixed at 90^o and evaluated in the ground state, for ^{16}O and ^{12}C, in Figure 2. All four graphs use as input one body reduced matrix elements from NCSM calculations with $N_{\max} = 18$ and $\hbar\omega = 20$ MeV based on the NNLO$_{\rm opt}$ interaction for the neutron distribution of ^{16}O (left panels) and ^{12}C (right panels). These two sets of calculations are very interesting, since while the scalar density looks similar in strength and distribution over the momenta for both nuclei, the spin-orbit contribution looks quite different. The maximum value of the spin-orbit contribution to the density is positive and about two order of magnitude smaller then the maximum value of the scalar density for ^{12}C, at about $q = 1$ fm^{-1} and $2\mathcal{K} = 1$ fm^{-1}, while for ^{16}O, the maximum value is negative and also about two order of magnitude smaller than the scalar one, at about $q = 0.7$ fm^{-1} and $2\mathcal{K} = 0.7$ fm^{-1}, and has another positive contribution distributed at different values of q and $\mathcal{K}$.

Looking at the absolute sizes of the scalar OBDs and the spin-orbit densities could lead to a conclusion that the latter being at least two orders of magnitude smaller may render them negligible in NA scattering calculations. For this consideration it is useful to recall the on-shell condition $\mathbf{q}^2 + \boldsymbol{\mathcal{K}}^2 = 4\mathbf{k_0}^2$ for NA scattering, where $\mathbf{k_0}$ is the on-shell momentum in the NA frame and related to the c.m. scattering energy. The on-shell conditions indicates that the maximum values on the scalar OBD close to the origin in Figures 1 and 2 are far off-shell in NA scattering. In Figure 3 we compare slices of the scalar and spin-orbit den-

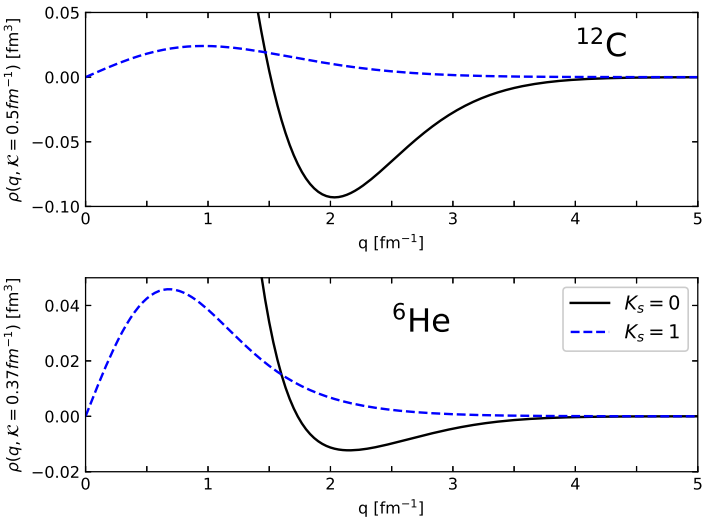

Figure 3. The expectation value of the scalar one-body density ($K_s = 0$) (solid) and the spin-orbit density ($K_s = 1$) (dashed) as function of the momentum transfer q for the fix value of $\mathcal{K}$=0.37 fm^{-1} (with the angle between them fixed at 90^o) for ^{6}He and $\mathcal{K}$=0.5 fm^{-1} for ^{12}C. The NCSM calculations were performed at $N_{\max}$=10 and $\hbar\omega$=20 MeV using the NNLO$_{\rm opt}$ interaction [18].

sities as function of q for fixed, small $\mathcal{K}$ values for ^{12}C and ^{6}He. Here we see that for q-values of about 1.5 fm^{-1} both densities have the similar values, and the effect on scattering observables may very well be visible. From Figure 3, we can also notice that the spin-density is relative constant in ^{12}C, while for ^{6}He has a maximum in momentum space at about 0.7 fm^{-1}, and goes to almost zero at about 2.5 fm^{-1} making the strength focused in momentum space, that mean spread out in coordinate space.

Since the reduced matrix elements of the one body operators calculated in NCSM are dependent of the parameter $N_{\max}$, we performed a series of calculations with different values of $N_{\max}$. We present in Figure 4 calculations of the expectation values of the spin-orbit operator ($K_s = 1$) as function of $\boldsymbol{q}$ and $\boldsymbol{\mathcal{K}}$, with the angle between them fixed at 90^o and evaluated in the ground state, for ^{4}He and ^{6}He, with $N_{\max} = 10$ and $N_{\max} = 18$. All four graphs use as input one body reduced matrix elements from NCSM calculations with $\hbar\omega = 20$ MeV. While the maximum contribution to the density is about 4.8×10^{-4} for ^{4}He with $N_{\max} = 10$, it increases only slightly to 4.9×10^{-4} for $N_{\max} = 18$. Interestingly, for ^{6}He, the strength of the spin-orbit contribution changes by about 15% (from 4.0×10^{-2} to 4.6×10^{-2}) when increasing the NCSM space from $N_{\max} = 10$ to $N_{\max} = 18$. By increasing $N_{\max}$, the strength of the distribution also moves slightly towards lower values of q and $\mathcal{K}$ for ^{6}He. Since including

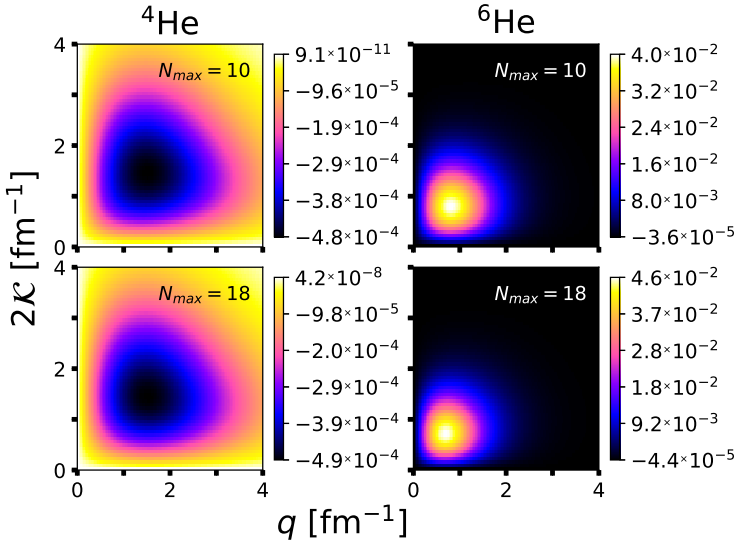

Figure 4. The neutron distribution of the spin-orbit operator expectation value, as a function of the momenta q and $\mathcal{K}$, with the angle between them fixed at 90^o, and evaluated in the ground state. The densities used as input the reduced matrix elements from NCSM calculations with two different values of $N_{\max} = 10$ and 18. All four calculations used input from NCSM with $\hbar\omega = 20$ MeV and are based on the NNLO$_{\rm opt}$ interaction [18] for ^{4}He (left panels) and ^{6}He (right panels).

more shells in the calculations drastically increasing the computation time, more calculations are underway in order to have a better understanding of how many shells are sufficient for converging results.

4 Summary and Outlook

We evaluated the expectation values of the scalar products of the spin of the struck target nucleon with its three linearly independent target momenta, $\hat{q}$, $\hat{\mathcal{K}}$, and $\hat{n}$. Only the expectation values of $\boldsymbol{\sigma}^{(i)} \cdot \hat{n}$, which correspond to the momentum representation of the spin-orbit operator, lead to a non-vanishing contribution. Our calculations indicate that for open-shell nuclei like ^{6}He and ^{12}C this spin-orbit density is considerably larger than for closed-shell nuclei like ^{4}He and ^{16}O. Since the spin-orbit density for the stuck target nucleon enters the NN scattering amplitude by means of the Wolfenstein amplitudes C and M, one may expect additional contributions to the traditional folding effective interaction for proton scattering of spin-zero nuclei in the central potential through the Wolfenstein amplitude C and in the spin-orbit potential through the Wolfenstein amplitude M. Corresponding work using the above developed expectation values is under way.

Acknowledgements

Partial support for this work is given by the U.S. DoE under DE-FG02-93ER40756, DE-SC0018223, DE-AC02-05CH11231, and the U.S. NSF under OIA-1738287, ACI-1713690, OCI-0725070, and ACI-1238993. G.P. acknowledges the support from the Ohio University Zanesville.

References

[1] P. Navratil, J.P. Vary, and B.R. Barrett, *Phys. Rev. Lett*. **84** (2000) 5728; arXiv:nucl-th/0004058.
[2] P. Navratil, J.P. Vary, and B.R. Barrett, *Phys. Rev. C* **62** (2000) 054311.
[3] R. Roth and P. Navratil, *Phys. Rev. Lett*. **99** (2007) 092501; arXiv:0705.4069.
[4] B. Barrett, P. Navrátil, and J. Vary, *Prog. Part. Nucl. Phys*. **69** (2013) 131.
[5] C. Stumpf, J. Braun, and R. Roth, *Phys. Rev. C* **93** (2016) 021301; arXiv:1509.06239.
[6] S.P. Weppner, O. Garcia, and C. Elster, *Phys. Rev. C* **61** (2000) 044601.
[7] A. Koning and J. Delaroche, *Nucl.Phys. A* **713** (2003) 231.
[8] T. Furumoto, K. Tsubakihara, S. Ebata, and W. Horiuchi, *Phys. Rev. C* **99** (2019) 034605.
[9] C.R. Chinn, C. Elster, and R.M. Thaler, *Phys. Rev. C* **48** (1993) 2956.
[10] C. Elster, T. Cheon, E.F. Redish, and P.C. Tandy, *Phys. Rev. C* **41** (1990) 814.
[11] R. Crespo, R.C. Johnson, and J.A. Tostevin, *Phys. Rev. C* **41** (1990) 2257.
[12] H.F. Arellano, F.A. Brieva, and W.G. Love, *Phys. Rev. C* **41** (1990) 2188; [Erratum: *Phys. Rev. C* **42** (1990) 1782].
[13] M. Burrows *et al.*, *Phys. Rev. C* **99** (2019) 044603; arXiv:1810.06442.
[14] M. Gennari, M. Vorabbi, A. Calci, and P. Navratil, *Phys. Rev. C* **97** (2018) 034619; arXiv:1712.02879.
[15] A. Orazbayev, C. Elster, and S.P. Weppner, *Phys. Rev. C* **88** (2013) 034610; arXiv:1305.6964.
[16] L. Wolfenstein and J. Ashkin, *Phys. Rev.* **85** (1952) 947.
[17] M. Burrows *et al.*, *Phys. Rev. C* **97** (2018) 024325; arXiv:1711.07080.
[18] A. Ekström *et al.*, *Phys. Rev. Lett*. **110** (2013) 192502.